Int j simul model 23 (2024) 1, 101-112
Original scientific paper

ANALYSIS OF FLOW STRAIGHTENER ON THE INTERNAL FLOW FIELD OF THREE-PHASE JET FIRE MONITORS

Zhang, X.; Ge, H. E.[#]; Liu, Z. & Liu, Y. Q.
College of Mechanical and Electronic Engineering, Shandong University of Science and Technology, Qingdao 266590, China
E-Mail: hongen_ge@sdust.edu.cn ([#] Corresponding author)

Abstract
To explore the influence of the flow straightener (FS) on the internal flow field of the three-phase jet fire monitor (TPJFM), this study conducted an analysis of the flow characteristics within the TPJFM. Through numerical simulations based on ANSYS/FLUENT, the velocity, turbulent kinetic energy, pressure, velocity uniformity, and outlet performance of the internal flow field of the TPJFM were evaluated for different FS installation positions, installation angles, and structures. Results show that, the structural form of the FS significantly influences the internal flow field. The advanced rectification capability of the FS can immediately return the fluid in the grid to a laminar flow state. However, the exchange of kinetic energy between the regions increases turbulent kinetic energy and reduces outlet velocity. The FS blade and symmetry plane of the powder pipe overlap can effectively reduce the turbulence kinetic energy generated by the powder pipe. Reasonable FS parameters can enhance the flow characteristics of the flow field and improve jet performance. These findings could serve as an important reference for designing an optimized TPJFM structure.
(Received in September 2023, accepted in January 2024. This paper was with the authors 3 weeks for 1 revision.)

Key Words: Three-Phase Jet Fire Monitor, Flow Characteristics, Flow Straightener, Internal Flow Field

1. INTRODUCTION

Fires are a grave threat to public safety and property, with over 3 million deaths worldwide attributed to urban fires alone annually [1]. Forest fires, mountain fires, and other major fires are escalating due to global warming and rising temperatures, leading to considerable loss of life and homes [2, 3]. At present, various fire extinguishing technologies have been applied in firefighting operations. The three-phase jet fire extinguishing technology can give full play to the performance advantages of various extinguishing agents with its high extinguishing efficiency and strong resistance to reignition. Such technology has been applied and rapidly developed for forests, chemical plants, and other key fire prevention places. The three-phase jet fire monitor (TPJFM) is the core equipment of three-phase jet fire extinguishing technology, and its performance seriously restricts its development. The internal flow field is essential for the circulation of water or other kinds of extinguishing agents, and its flow characteristics are vital to determining the overall performance. The analysis and exploration of the flow characteristics of the TPJFM are crucial research problems that require attention to improve the three-phase jet fire extinguishing technology.

Unlike traditional fire monitors, TPJFMs can handle solid-liquid-gas three-phase composite jets during operation and thus require a powder pipe for fire monitor insertion. The fluid that encounters obstacles in the flow process is susceptible to turbulence, swirl, and other forms of unstable flow. This phenomenon is particularly pronounced in the case of inclined cylinders, resulting in a heightened disorder in vortex shedding [4]. Moreover, elevating the angle of inclination of the cylinder attenuates the three-dimensional characteristics of the flow, as detailed in [5]. Research on circular pipe flow has shown that installing a splitter plate in the pipe significantly reduces turbulent fluctuations at the outlet, and the location and structure of the splitter plate are critical in eliminating unsteady flow [6]. The widely used Zanker plate is

a flow straightener (FS) that eliminates turbulence from tubing for experimental fluid flow applications [7]. FS corrects the direction of liquid flow, eliminates the energy loss caused by unstable flow such as swirls, and enhances outlet velocity and flow distribution. Therefore, exploring the influence of FS on the internal flow field and flow characteristics of TPJFMs should be examined to improve the jet performance of TPJFMs.

This study explores the flow effect of the FS by analysing the influence of its installation position, installation angle, and structural form on the average velocity, velocity distribution, turbulent kinetic energy, turbulent kinetic energy distribution, and velocity uniformity of the internal flow field of the TPJFM. The FS is intended to reduce the turbulent kinetic energy, increase outlet velocity, improve the quality of the outlet velocity distribution, and provide theoretical support for optimizing the jet performance of the TPJFM.

2. STATE OF THE ART

Some scholars have examined the impact of modifications in the structure, position, and other parameters of the FS system. Xiang et al. [8] conducted multi-objective optimization using a hybrid multi-objective genetic algorithm on the traditional fire monitor's FS. They selected the length of the FS, the blade thickness, and the outer tube radius as the design parameters to improve the jet range of the fire monitor. The study established that the structural and installation parameters of the FS significantly impact the outlet speed and fluctuation of the fire monitor.

Some scholars have examined the role of FS in other fluids. Negash et al. [9] investigated the combined effect of the position and porosity of the FS on the waste heat recovery performance of a thermoelectric generator. Daev and Kairakbaev [10] proposed a model for determining liquid flow in a tube containing the FS, considering the influence of FS parameters on the liquid flow measurement process. Seo [11] found that the turbulence intensity decreases with a reduction of FS's hydraulic diameter. Research has demonstrated that the parameters of the FS significantly improve flow characteristics, such as the correction and velocity distribution of the fluid. Considerable research has been conducted on improving the flow channel structure in fire monitors and the nozzle performance, primarily focusing on simulation and experimentation. Based on the vorticity field, Xi et al. [12] studied the flow characteristics of the side pump sum with FLUENT. Results show that the inflow distribution is uneven and the water flow resistance and vortex strength are imbalanced due to the asymmetry of the vorticity of the inflow of the side pump sump. Min and Cho [13] designed a new fire nozzle structure and analysed it with finite elements. Song et al. [14] compared and examined the velocity distribution of the flow field and the impact pressure on the target surface of four different structure nozzles, showing that the conical short-line nozzle exhibits better jet convergence and stability. After analysing nozzle jet speed, nozzle angle, nozzle pressure, and nozzle size on the tinplate temperature field, Zhang et al. [15] found that the appropriate nozzle structure and flow parameters could increase the uniformity of the tinplate temperature field. Jiang et al. [16] demonstrated that the convergence angle and straight section length of the nozzle significantly impact the hydraulic performance of the nozzle. Hou et al. [17] designed a liquid nitrogen water fire monitor nozzle and examined the effects of its rectifier tube and constriction angle on the jet. Wen et al. [18] used numerical simulations and experiments to obtain the optimal structural parameters of a straight cone nozzle. The results showed that the cylindrical outlet cross-section of the straight cone nozzle improves its hydraulic performance. Moreover, the main research object is the traditional direct-flow fire monitor. Jia [19] designed a TPJFM with a powder pipe in the centre, optimized its main structural parameters individually, and obtained a set of optimal structural parameter combinations. However, the effect of the FS on the flow characteristics was not addressed while optimizing the TPJFM

nozzle structure. Previous studies have extensively focused on improving fluid flow characteristics by FS. However, analysis and research on the impact of FS on the internal flow characteristics of TPJFM have been limited. While previous research has concentrated on the influence of FS on the internal flow field, mainly focusing on traditional fire monitors and other fluid structures, research on the FS of TPJFMs has not been conducted. Therefore, the present study establishes the flow model of the internal flow channel of TPJFM through numerical simulation. This study also analyses the influence of the FS on the internal flow field of the TPJFM by combining the change of the parameters of the FS and the influence of the FS parameters on the flow characteristics of the internal flow field. The findings provide a theoretical basis for future optimization of the internal flow channel structure of the TPJFM and the improvement of jet flow performance.

The rest of this study is organized as follows. Section III describes the structure of the TPJFM, extracts and meshes the flow domain, verifies the mesh independence, and sets boundary conditions. Section IV analyses the influence of the installation position, installation angle, and structural form of the FS on the internal flow field of the TPJFM. Section V summarizes the study and draws relevant conclusions.

3. METHODOLOGY

3.1 TPJFM model

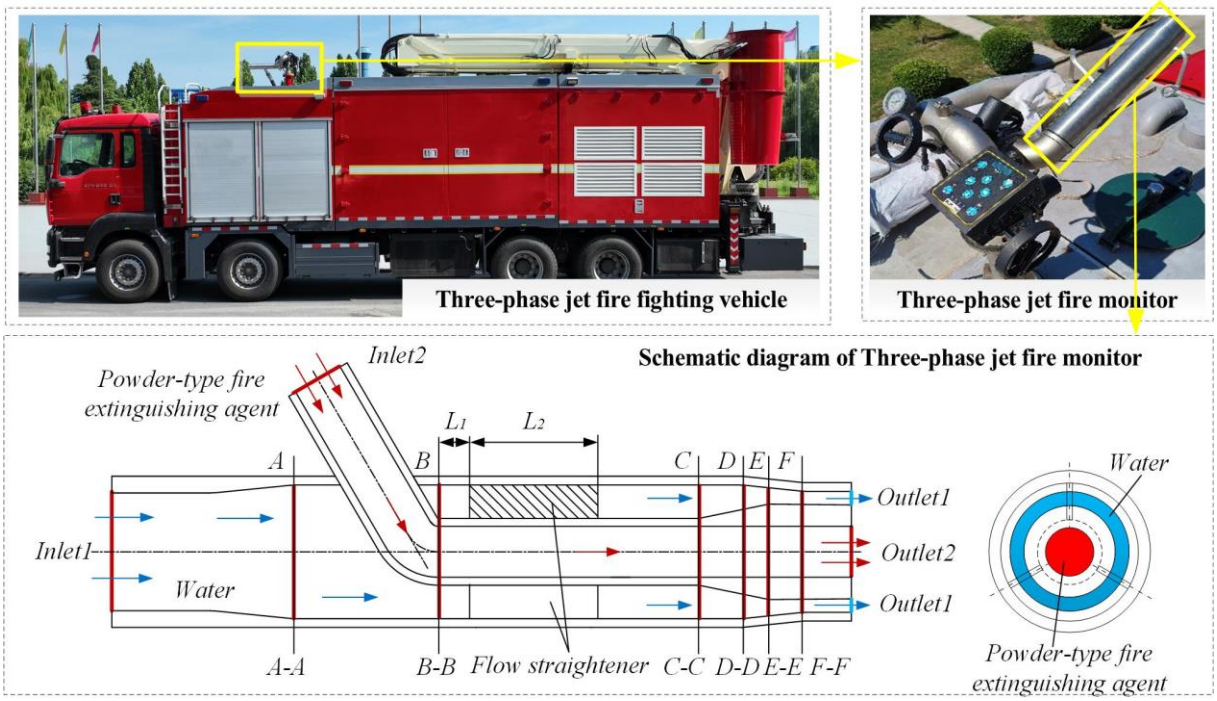

Figure 1: Schematic structure of TPJFM.

The TPJFM consists of a water pipe, a powder pipe, and an FS. The structure is shown in Fig. 1. The water pipe is the main flow channel through which liquid types of extinguishing agents pass, and the powder pipe is the auxiliary flow channel through which powders, gases, and other types of extinguishing agents pass. Liquid fire extinguishing agents jet out of the nozzle at high speed in a water ring state. After moving for a certain distance, the powder extinguishing agent is mixed, carried, and sprayed from the powder pipe, and the fire source continues to move for firefighting operations. The internal flow channel of the TPJFM mainly consists of the outer wall of the powder pipe, the inner wall of the water pipe, and the FS. The powder pipe is inserted into the centre of the flow channel at a 120° inclination, and the internal

flow field region shrinks as it passes through C, D, E, and F, culminating in the schematic at the outlet shown on the right of Fig. 1.

3.2 Volume of fluid (VOF) theoretical model and boundary conditions

In this study, the air-water interface was tracked using a VOF model under a fixed Eulerian grid [20], and the VOF transport equation:

$$\frac{\partial \gamma}{\partial t} + (\boldsymbol{u} \cdot \nabla)\gamma = 0 \tag{1}$$

where γ is the fractional function, $\gamma = 0$ means no air in the flow field, $\gamma = 1$ means only air in the flow field, $0 < \gamma < 1$ means air and water phases in the flow field. The grid has a gas-liquid interface; $\boldsymbol{u}$ is the velocity, m/s; t is the time, s.

The VOF model solves a single momentum equation within the entire solution domain, and the air and water phases share the solved velocity field. The mass and momentum equations are as follows:

$$\frac{\partial \bar{\rho}}{\partial t} + \nabla \cdot \left(\bar{\rho}\boldsymbol{u}\right) = 0 \tag{2}$$

$$\frac{\partial}{\partial t}\left(\bar{\rho}\boldsymbol{u}\right) + \nabla \cdot \left(\bar{\rho}\boldsymbol{u}\boldsymbol{u}\right) = -\nabla p + \nabla \cdot \left[\bar{\mu}\left(\nabla \boldsymbol{u} + \nabla \boldsymbol{u}^T\right)\right] + \bar{\rho}g + \boldsymbol{F} \tag{3}$$

where g is the acceleration of gravity, m/s^2; p is the pressure, Pa; $\bar{\rho}$ is the equivalent density, kg/m^3; $\bar{\mu}$ is the equivalent viscosity, Pa·s.

The pressure-based steady-state computational model is used. Pressure-inlet, pressure-outlet, standard k-epsilon model, standard wall function, the convergence residuals of 10^{-4}, the Coupled algorithm are used, and the momentum, turbulence kinetic energy, and turbulence dissipation rate are used in the second order upwind. The inlet pressure is 0.8 MPa, the outlet pressure is 0, and the iterative calculation is stopped when each parameter converges below the set residual.

The relative standard deviation SV is a dimensionless value to characterize the relative variability, which is used to characterize the uniformity of fire monitor cross-section velocities. The uniformity of the flow field in the cross-section is judged by comparing the SV values under different working conditions, and the smaller the SV value, the higher the uniformity of the flow field.

$$SV = S / \bar{V} \times 100\% \tag{4}$$

$$S = \sqrt{\frac{1}{n-1}\sum_{j=1}^{n}(V_j - \bar{V})^2} \tag{5}$$

where S is the standard deviation; V_j is the velocity value of the j sampling point; $\bar{V}$ is the average velocity of all sampling points; and n is the number of sampling points.

4. RESULT ANALYSIS AND DISCUSSION

4.1 Influence of FS installation position on the flow characteristics of the TPJFM

In the traditional fire monitor structure, the FS can effectively reduce the flow other than axial flow so that more energy can be converted into the outlet's kinetic energy. The TPJFM causes a sharp increase in turbulent kinetic energy due to the obstruction of the powder pipe to the fluid division. With the structural form of the FS and the installation angle unchanged, the distance of the FS from the powder pipe is changed to analyse the influence of the position of the FS on the flow characteristics of the flow field in the fire monitor.

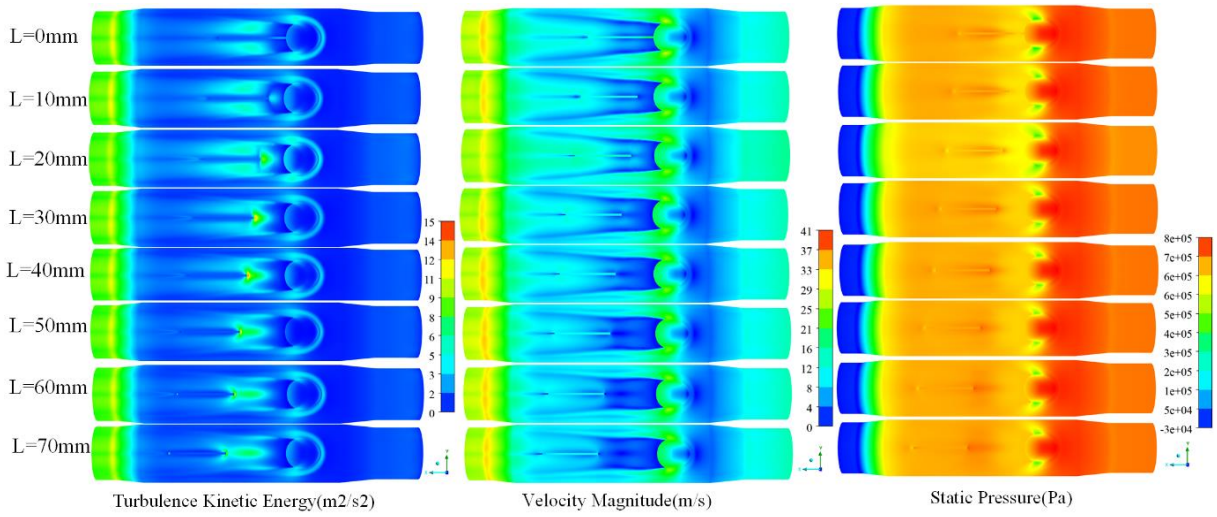

Figure 2: Overall cloud diagram of FS at different installation positions.

From the cloud analysis of turbulent kinetic energy in Fig. 2, as the distance between the FS and the powder pipe increases, the distribution area of turbulent kinetic energy gradually concentrates from dispersion, and turbulent kinetic energy concentration points are seen when the fluid contacts the FS blades at 30, 40, and 50 mm. Areas of concentration disperse as the distance continues to increase. From the velocity cloud diagram, with the increase of the distance, the velocity of the back side region of the powder pipe gradually decreases, and the velocity distribution appears uneven, making the back side region of the powder pipe show instability. The pressure distribution is relatively small, with concentrated areas on both sides of the powder tube. As the distance increases, the pressure concentration area gradually becomes concentrated, and the position gradually moves back.

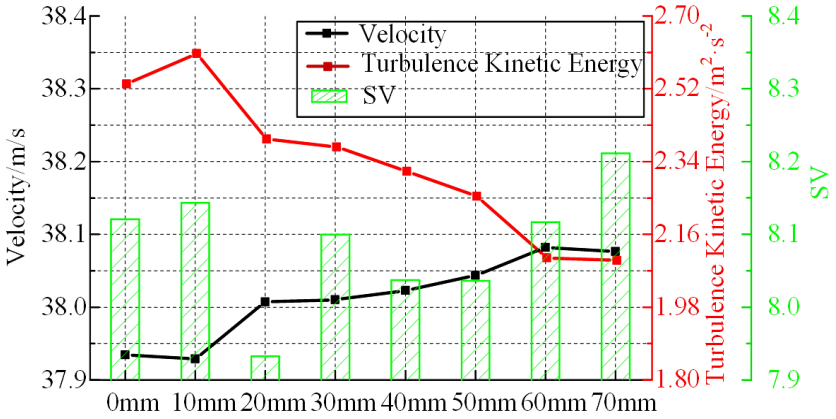

Figure 3: Performance of fire monitor outlet.

According to the average velocity at the outlet of Fig. 3, as the installation position of the FS moves backward, the average velocity gradually increases. At the distance of 10 mm from the FS to the powder pipe, the minimum average velocity at the outlet is 37.9 m/s and at 60 mm, and the average velocity is a maximum of 38.1 m/s, which is an increase of 0.2 m/s or 0.53 %. Turbulent kinetic energy is increased and then decreased with the increase of the distance, and the turbulent kinetic energy is maximized to 2.61 $m^2 \cdot s^{-2}$ at 10 mm and minimized to 2.10 $m^2 \cdot s^{-2}$ at 60–70 mm, which is decreased by 7.5 %. Velocity uniformity shows irregular fluctuations, with the best uniformity of 7.93 at 20 mm and the lowest uniformity of 8.21 at 70 mm, which is a 3.5 % decrease.

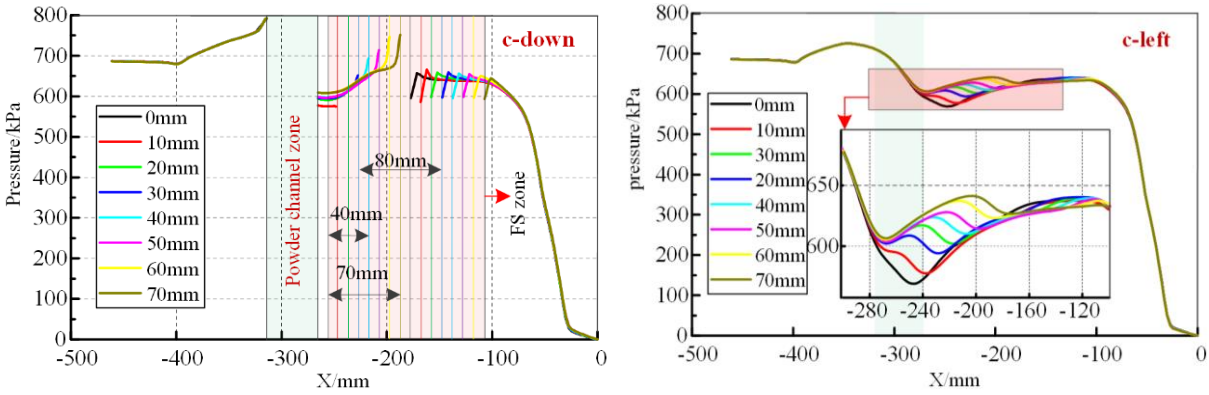

Figure 4: Variation of the c-down (left) and c-left (right) pressure of the internal flow field.

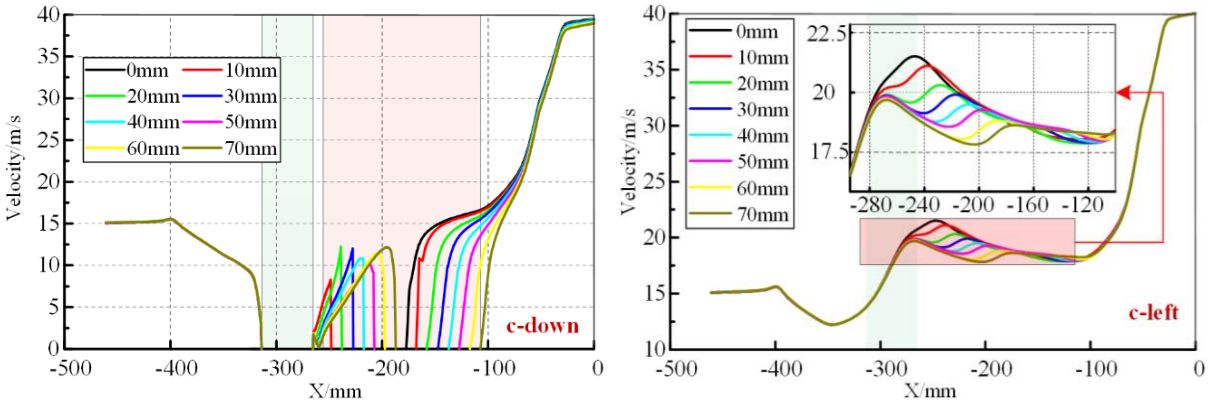

Figure 5: Variation of the c-down (left) and c-left (right) velocity of the internal flow field.

Longitudinal lines are inserted in the internal flow field at the up, down, and left sides, and the flow data on the lines are extracted to analyse the flow characteristics of the internal flow field. From Fig. 4, the effect of the FS installation position on the pressure in the fluid region at the front side of the powder pipe is negligible, all gradually increasing. For the fluid behind the powder pipe, as the FS moves away from the powder pipe, the pressure gradually increases and reaches its maximum value when in contact with the FS blades. Given the function of the FS, the pressure in the down area behind the FS increases to a certain value and gradually decreases. From the variation of pressure in the up region of the internal flow field with *X*, the variation of up pressure with the position of the FS is relatively small. According to the analysis of the changes in pressure on the left and right sides of Fig. 5, as the installation position of the FS moves away, the pressure fluctuation on the rear side of the powder pipe gradually decreases.

From the velocity changes in the downside of the internal flow field in Fig. 5, the velocity fluctuation is minimized at 50 mm with increased distance between the FS and the powder pipe. The velocity fluctuation in the up region gradually increases with the backward shift of the installation position of the FS, which further proves that the presence of the FS can effectively suppress the fluctuation generation and stabilize the turbulent flow rapidly. From the velocity and pressure of the left side of the internal flow field in Figs. 5 and 4, the FS away from the powder pipe can gradually reduce the amplitude of the oscillation of the velocity, effectively improving the stability of the fluid in the internal flow field.

According to the variation of turbulent kinetic energy in Fig. 6, as the distance increases, the turbulent kinetic energy between the powder pipe and the FS fluctuates sharply, peaking at 50 mm from the FS to the powder pipe. As the distance increases, the turbulence kinetic energy fluctuations in the down region show an overall increasing trend. From the analysis of turbulent kinetic energy in the left region, the fluctuation amplitude of turbulent kinetic energy in the

outlet region decreases and tends to flatten out as the distance increases. The turbulent kinetic energy in the region between the blades of the stabilizer decreases as the distance increases.

Based on the above analysis, turbulent kinetic energy is negatively correlated with velocity, and reducing the generation of turbulent kinetic energy in the internal flow field is necessary to increase outlet velocity. Reasonable planning of the installation position of the FS can increase the velocity uniformity of the outlet and increase the distance of the fire monitor jet. The premature correction of turbulence due to blunt body bypassing by the FS causes a decrease in velocity uniformity, and the exchange of energy between the various regions after passing through the FS causes an increase in turbulent kinetic energy.

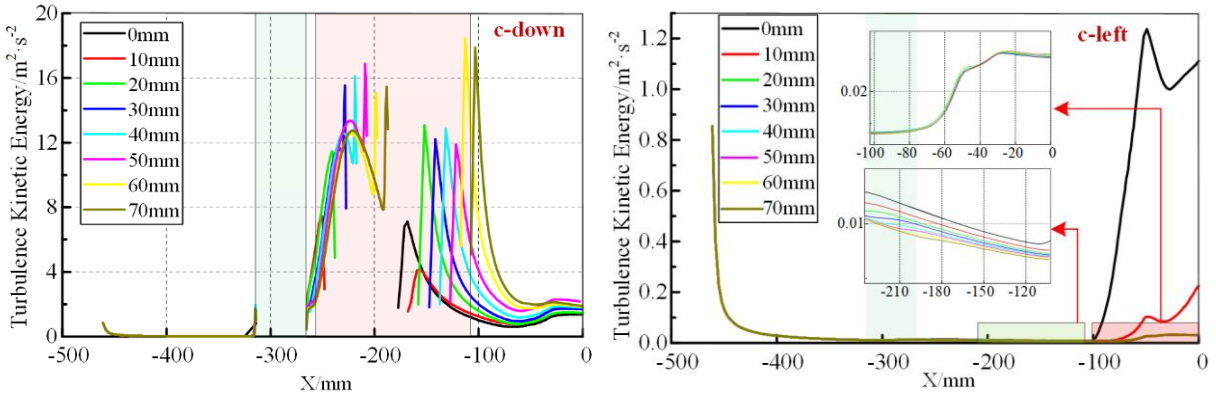

Figure 6: Variation of the c-down (left) and c-left (right) turbulent kinetic energy of the internal flow field.

4.2 Effect of the number of blades on flow characteristics of the TPJFM

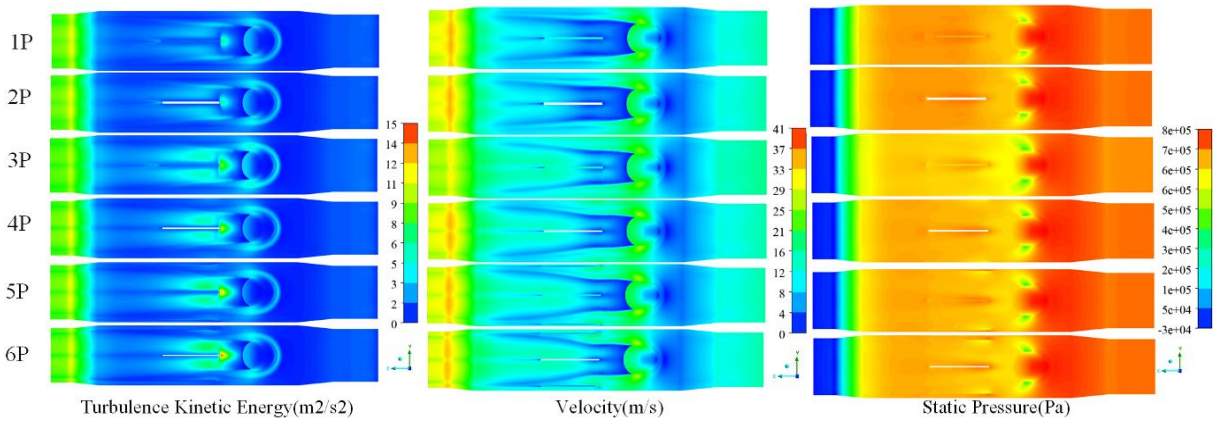

Figure 7: Overall cloud diagram of FS in different forms.

The structural form of the FS can effectively change the flow distribution state of the fluid and affect the streamline inclination and helicity of the flow field. Given the structural complexity of the TPJFM, the structural form of the FS has some limitations. Therefore, under the condition of ensuring the same cross-sectional area of the FS, the number of pieces of the FS is increased to study the effect of different forms of the FS on the flow characteristics of the flow field in the TPJFM. The design FS structure form 1P, 2P, 3P, 4P, 5P, and 6P, totalling six types. The installation angle is 0°, the symmetry surface of a piece of the FS and the powder pipe symmetry surface overlap, and the FS is installed 20 mm away from the powder pipe.

From the overall cloud diagram of Fig. 7, the divided fluid region increases with the increase in the number of FS blades. The turbulent kinetic energy in the reign of contact between the rear side of the powder pipe and the FS blades appears to be concentrated, and the distribution of turbulent kinetic energy between the FS blades becomes larger. Velocity shows an increasing

trend in the overall distribution on the back side of the powder pipe, with less variation in the pressure cloud maps. The change in the region of velocity distribution and turbulent kinetic energy is mainly due to the increase in the splitting region, which results in the high-velocity flow of the powder pipe bypass immediately entering into the splitting region without exchanging kinetic energy. The flow distribution on the upper side is relatively large, leading to a concentration point of turbulent kinetic energy and an increase in velocity in the rear region.

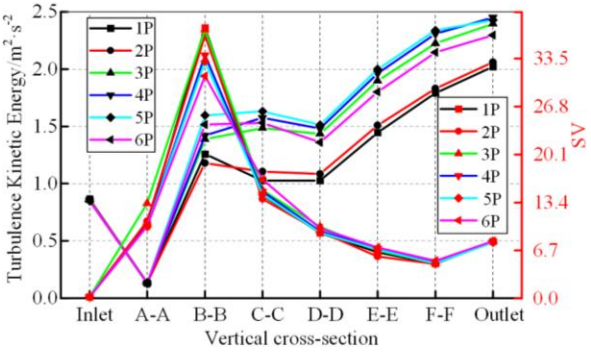

Figure 8: Turbulent kinetic energy and velocity uniformity of cross-sections.

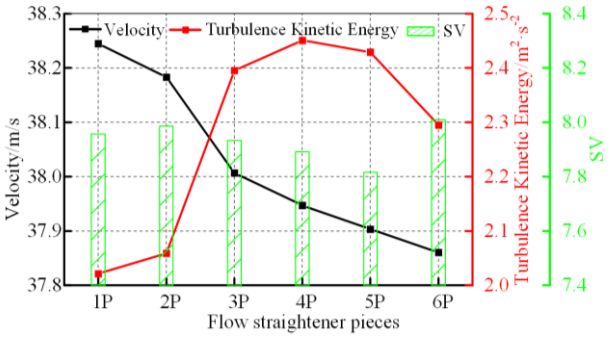

Figure 9: Performance of fire monitor outlet.

Table I: Differential pressure between sections in different forms, /kPa.

FS form	1P	2P	3P	4P	5P	6P
A-B	116.5	114.9	115	114.1	113.8	114.5
A-C	76.3	79.8	86.3	87.4	89.0	92.3
B-C	−40.2	−35.1	−28.7	−26.7	−24.8	−22.2

According to Fig. 8, the turbulent kinetic energy of each cross-section shows an increasing trend with the increase in the number of blades, and the turbulent kinetic energy of each cross-section is the maximum at five blades. Velocity uniformity increases in section B-B, but section C-C at the back side of the FS tends to decrease uniformity with an increasing number of blades. Therefore, the unreasonable increase in the number of blades will increase the generation of turbulent energy in the internal flow field, and the reasonable partition region can increase the flow stability of the internal flow field.

From the analysis of Table I, the differential pressure between A-C increases gradually, and the pressure loss rises gradually as the number of blades increases. The maximum differential pressure is 92.3 kPa when there are six blades, which is 20.8 % higher than when there is one blade. The cross-sectional pressure difference between B-C has also increased, indicating that the pressure loss between B-C is also intensifying. Although the water retaining area of the blades remains constant when designing the number of blades, the pressure loss because of the wall and the turbulence energy is still unavoidable. Thus, reducing the number of blades is beneficial to minimize the pressure loss.

The outlet velocity decreases linearly with the increased number of FS blades. The average outlet velocity is 38.24 m/s when the FS is 1P to 37.86 m/s when the FS is 6P. The average velocity decreases by 0.38 m/s. Turbulence kinetic energy decreases with the increase of the blades to the highest point. The turbulence kinetic energy is maximum at 4P, which is 2.45 $m^2 \cdot s^{-2}$, and increases by 21.3 % compared with the minimum value of 1P, which is 2.02 $m^2 \cdot s^{-2}$. With the increase of the number of blades the uniformity of the velocity shows an increasing, decreasing, and then increasing trend, the best uniformity is 7.81 at 5P compared to 8.01 at 6P, where the uniformity is poor and the uniformity of the velocity decreases by 2.5 %. Therefore, increasing the number of blades can increase the uniformity of the outlet velocity to

some extent and make the outlet velocity more stable. However, the increase in the number of blades increases the pressure drop, and the average outlet velocity further decreases.

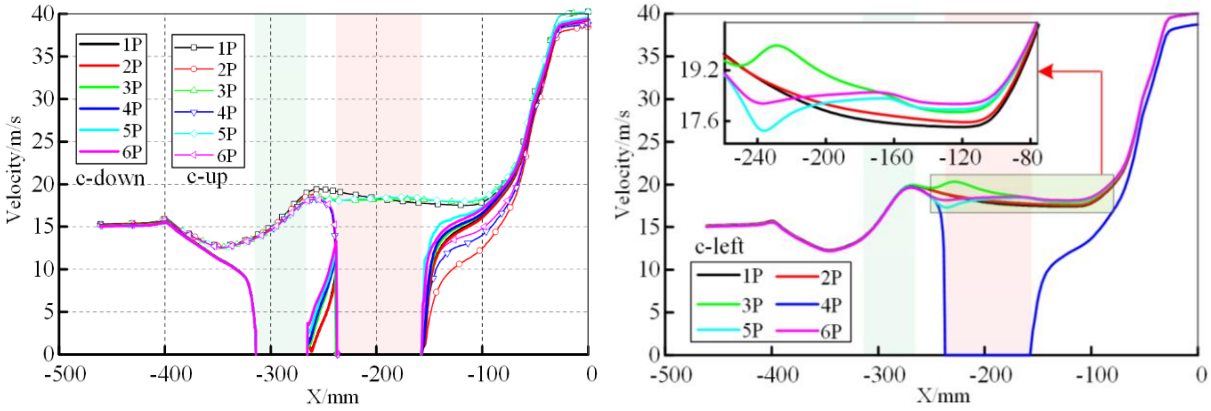

Figure 10: Variation of the c-down (left) and c-left (right) velocity of the internal flow field.

According to the analysis of Fig. 10, the increase in velocity and the growth rate increases with the increase in the number of blades in the upper and lower side regions at the rear of the FS, but the difference fades away closer to the outlet. In the left side velocity distribution, with the increase in the number of blades, the fluctuation of the velocity in the front side of the FS is increased, and the velocity after the FS is corrected is elevated. Given the increased number of blades, the disturbed fluid is forced into the FS before it is smooth, and the velocity fluctuates. Subsequently, the FS corrects the resulting fluctuations in a timely manner, eliminating the velocity fluctuations caused by the turbulent flow, and the velocity gradually levels off.

The increase in the number of blades affects the flow of fast water on the upper side of the internal flow field to the lower side of the lower region of the lower flow velocity. Although such effect corrects to some extent the fluid in other directions except the longitudinal flow, the velocity of the entire internal flow field region is distributed regionally and reduces the velocity uniformity of the outlet. In the TPJFM, the increase in the number of blades exacerbates the pressure loss in the internal flow field, reduces the average velocity at the outlet, and exacerbates turbulent kinetic energy generation.

4.3 Effect of installation angle on flow characteristics inside a TPJFM

The installation angle of the FS also affects the flow characteristics of the internal flow field of the TPJFM, which further affects the velocity and velocity uniformity at the outlet. This study analyses the impact of installation angles of three-blade FS at 0 d, 30 d, 60 d, and 90 d (degrees) on the flow characteristics of the internal flow field of the fire monitor.

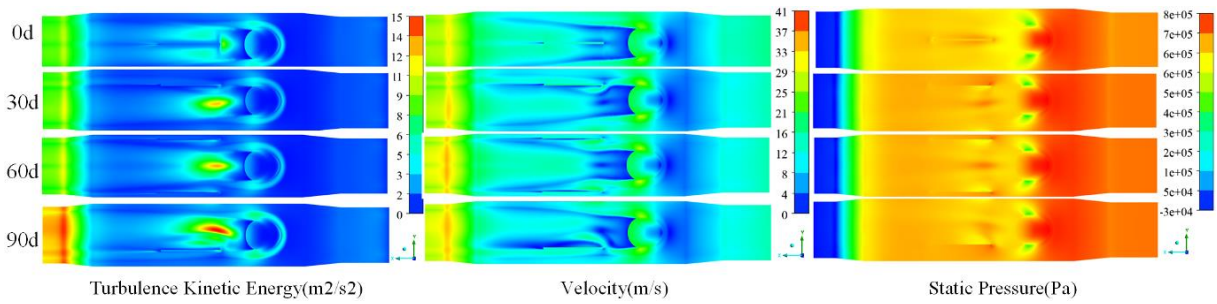

Figure 11: Overall cloud diagram of FS at different installation angles.

According to Fig. 11, as the installation angle increases, the region of turbulent kinetic energy gradually increases and becomes more concentrated in the FS region behind the powder

pipe. From the velocity cloud map, the symmetrical installation angle of the FS can effectively eliminate lateral flow, the velocity distribution is more reasonable and smooth, and the fluid division region is more reasonable. The analysis shows that an excessively small angle between the powder pipe and the FS causes a sharp increase in turbulent kinetic energy, affecting the overall flow performance.

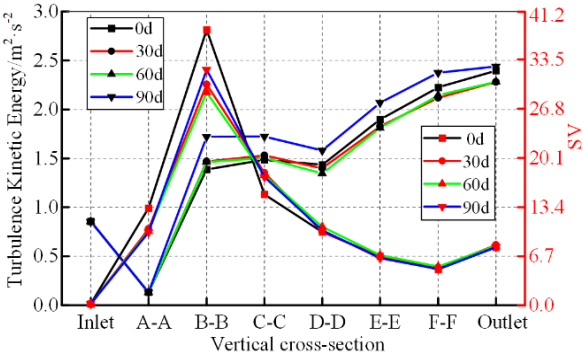

Figure 12: Turbulent kinetic energy and velocity uniformity of cross-sections.

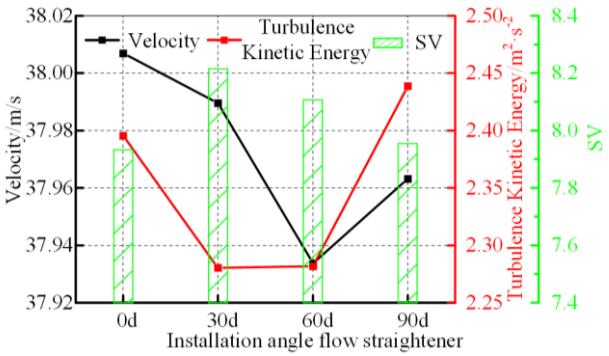

Figure 13: Performance of fire monitor outlet.

According to Fig. 12, the average turbulent kinetic energy of the cross-section in the section after the B-B section is at its maximum at the installation angle of 90 d. Behind the powder pipe, the 30 d and 60 d variations are essentially the same and lower than the 0 d mean value. The analysis of velocity uniformity for each cross-section shows that the installation angle of the FS had the greatest effect on the velocity uniformity of the B-B. The uniformity is worst at 0 d and better at 60 d. Given the different installation angles of the FS, the flow capacity is affected while further affecting the velocity uniformity of the internal flow field.

Different installation angles for outlet performance parameters are shown in Fig. 13. The velocity decreases and then increases with the increase of the installation angle. The average velocity is a minimum of 37.93 m/s at 60 d and a maximum of 38.0 m/s at 0 d, and the change of installation angle of FS has less effect on the outlet velocity. The minimum turbulent kinetic energy is 2.28 $m^2 \cdot s^{-2}$ at 30 d and 60 d, whereas the maximum turbulent kinetic energy is only reduced by 0.11 $m^2 \cdot s^{-2}$. The fluctuation range of uniformity is 0.28. Therefore, the change of installation angle has less effect on the performance of the fire monitor outlet.

5. CONCLUSION

The influence of the installation position, installation angle, and structural form of the FS on the average velocity, turbulence kinetic energy, and velocity uniformity of the internal flow field of the TPJFM were analysed to improve the jet performance of TPJFM and study the influence of FS on the flow characteristics of the internal flow field of TPJFM. The following conclusions were drawn:

(1) As the distance between the FS and the powder pipe increases, the average velocity of the outlet increases, and the turbulent kinetic energy decreases. When the distance is 60 mm, the velocity increases by 0.2 m/s, and the turbulent kinetic energy decreases by 7.5 %. Early rectification can make the water fluid in the FS grid return to the laminar flow state quickly. However, the premature correction of the laminar flow around the blunt body will lead to a decrease in the uniformity of the outlet velocity, an increase in the turbulent kinetic energy, and a decrease in the velocity.

(2) With FS blades increasing, the outlet's velocity decreases, the pressure loss in the internal flow field rises, and the turbulent kinetic energy increases and then decreases. With one FS blade, the velocity increases by 0.38 m/s, and the turbulent kinetic energy decreases by

17.6 %. The increase in the number of blades raises the fluid partitioning in the flow channel. Thus, this increase affects the flow from the upper part of the internal flow field, where the velocity is fast, to the lower region, where the velocity is low. However, it makes the flow distribution more uneven and decreases uniformity.

(3) Compared with the installation position and structure form, the installation angle of the FS has less influence on the performance of the fire monitor outlet, the FS blade, and the symmetry plane of the powder pipe overlap. It can eliminate the asymmetrical phenomenon of splitting the fluid area brought about by the installation angle, reduce the turbulent kinetic energy, and improve the flow characteristics of the internal flow field.

Reasonable FS structure, installation position, and angle can reduce the outlet's turbulent kinetic energy, increase the outlet velocity, and improve the fire monitor jet performance. However, the present study does not consider whether the changes between the FS parameters have other influences on the influence law. The next study can comprehensively investigate the change of various influencing parameters on the flow field inside the TPJFM by designing multifactor parameters tests.

ACKNOWLEDGEMENT

This study was supported by the key research and development of Shandong province, China (Grant No. 2019SDZY01).

REFERENCES

[1] Bispo, R.; Vieira, F. G.; Bachir, N.; Espadinha-Cruz, P.; Lopes, J. P.; Penha, A.; Marques, F. J.; Grilo, A. (2023). Spatial modelling and mapping of urban fire occurrence in Portugal, *Fire Safety Journal*, Vol. 138, Paper 103802, 9 pages, doi:10.1016/j.firesaf.2023.103802

[2] Ladds, M.; Keating, A.; Handmer, J.; Magee, L. (2017). How much do disasters cost? A comparison of disaster cost estimates in Australia, *International Journal of Disaster Risk Reduction*, Vol. 21, 419-429, doi:10.1016/j.ijdrr.2017.01.004

[3] Baena, J. C.; Wang, C.; Kabir, I. I.; Khalid, A.; Nazir, M. T.; Yuen, A. C. Y.; Ahmad, F.; Yeoh, G. H. (2023). Fire behaviour of waterborne intumescent coatings on timber substrate for bushfire exposure, *Fire Safety Journal*, Vol. 140, Paper 103836, 10 pages, doi:10.1016/j.firesaf.2023.103836

[4] Hogan, J. D.; Hall, J. W. (2010). The spanwise dependence of vortex-shedding from yawed circular cylinders, *Journal of Pressure Vessel Technology*, Vol. 132, No. 3, Paper 031301, 5 pages, doi:10.1115/1.4000732

[5] Thapa, J.; Zhao, M.; Zhou, T. M.; Cheng, L. (2014). Three-dimensional simulation of vortex shedding flow in the wake of a yawed circular cylinder near a plane boundary at a Reynolds number of 500, *Ocean Engineering*, Vol. 87, 25-39, doi:10.1016/j.oceaneng.2014.05.014

[6] Xiang, Q. J.; Liu, J.; Ye, D. X.; Wang, X. K. (2022). Influence of splitter plate on the hydraulic performance of the curved barrel of firefighting water cannon, *Journal of Mechanical Science and Technology*, Vol. 36, No. 2, 775-784, doi:10.1007/s12206-022-0125-7

[7] El Drainy, Y. A.; Saqr, K. M.; Aly, H. S.; Mohd Jaafar, M. N. (2014). CFD analysis of incompressible turbulent swirling flow through Zanker plate, *Engineering Applications of Computational Fluid Mechanics*, Vol. 3, No. 4, 562-572, doi:10.1080/19942060.2009.11015291

[8] Xiang, Q.-J.; Xue, L.; Kim, K.-Y.; Shi, Z.-F. (2019). Multi-objective optimization of a flow straightener in a large capacity firefighting water cannon, *Journal of Hydrodynamics*, Vol. 31, No, 1, 137-144, doi:10.1007/s42241-019-0018-0

[9] Negash, A. A.; Choi, Y.; Kim, T. Y. (2021). Experimental investigation of optimal location of flow straightener from the aspects of power output and pressure drop characteristics of a thermoelectric generator, *Energy*, Vol. 219, Paper 119565, 12 pages, doi:10.1016/j.energy.2020.119565

[10] Daev, Z. A.; Kairakbaev, A. K. (2017). Measurement of the flow rate of liquids and gases by means of variable pressure drop flow meters with flow straighteners, *Measurement Techniques*, Vol. 59, No. 11, 1170-1174, doi:10.1007/s11018-017-1110-x

[11] Seo, Y. (2013). Effect of hydraulic diameter of flow straighteners on turbulence intensity in square wind tunnel, *HVAC&R Research*, Vol. 19, No. 2, 141-147, doi:10.1080/10789669.2012.749133
[12] Xi, W.; Lu, W. G.; Wang, C.; Liu, J. F. (2022). Analysis of pumping station inlet characteristics based on vorticity, *International Journal of Simulation Modelling*, Vol. 21, No. 3, 453-464, doi:10.2507/IJSIMM21-3-610
[13] Min, D. L.; Cho, H. Y. (2021). Fire nozzle internal shape design to reduce anti repulsive force, *Transactions of the Korean Society of Mechanical Engineers – A*, Vol. 45, No. 8, 699-707, doi:10.3795/ksme-a.2021.45.8.699
[14] Song, G. F.; Zheng, H. X.; Wang, Y. N.; Zheng, Y. Y.; Zhou, Y.; Yao, B. (2019). Finite element analysis of nozzle selection based on high pressure water jet technology, *IOP Conference Series: Earth and Environmental Science*, Vol. 267, No. 4, Paper 042053, 7 pages, doi:10.1088/1755-1315/267/4/042053
[15] Zhang, W. J.; Zhang, X. D.; Guo, Z. F.; Wang, J. H.; Bai, Z. H. (2023). Simulation analysis of temperature field of tinplate in the quenching, *International Journal of Simulation Modelling*, Vol. 22, No. 1, 88-99, doi:10.2507/IJSIMM22-1-634
[16] Jiang, T. W.; Huang, Z. W.; Li, J. B.; Zhou, Y. S.; Xiong, C. (2022). Effect of nozzle geometry on the flow dynamics and resistance inside and outside the cone-straight nozzle, *ACS Omega*, Vol. 7, No. 11, 9652-9665, doi:10.1021/acsomega.1c07050
[17] Hou, Y.; Yang, X.; Ren, F.; Liu, Y. (2018). Structural analysis and optimization of liquid nitrogen fire monitor based on FLUENT, *Proceedings of the 3rd International Conference on Electrical, Automation and Mechanical Engineering (EAME 2018)*, 295-299, doi:10.2991/eame-18.2018.62
[18] Wen, J. W.; Qi, Z. W.; Behbahani, S. S.; Pei, X. J.; Iseley, T. (2019). Research on the structures and hydraulic performances of the typical direct jet nozzles for water jet technology, *Journal of the Brazilian Society of Mechanical Sciences and Engineering*, Vol. 41, No. 12, Paper 570, doi:10.1007/s40430-019-2075-2
[19] Jia, C. D. (2019). *Structural Design and Performance Study of the Three-Phase Jet Fire Monitor*, Master Thesis, China University of Mining and Technology, Xuzhou (in Chinese)
[20] Hirt, C. W.; Nichols, B. D. (1981). Volume of fluid (VOF) method for the dynamics of free boundaries, *Journal of Computational Physics*, Vol. 39, No. 1, 201-225, doi:10.1016/0021-9991(81)90145-5